This is a preproof accepted article for *Mineralogical Magazine*
This version may be subject to change during the production process
DOI: 10.1180/mgm.2025.10143

Revision 2

Article

Boevskite, $Pb_4(TeO_3)_2(SO_4)(S_2O_3)$, the first mixed sulfate–thiosulfate mineral from the Boevskoe deposit, Southern Urals, Russia

Anatoly V. Kasatkin[1], Natalia V. Zubkova[2], Radek Škoda[3]*, Vladislav V. Gurzhiy[4], Fabrizio Nestola[5], Cristian Biagioni[6], Atali A. Agakhanov[1], Sergey N. Britvin[4], Jakub Plášil[7], and Aleksey M. Kuznetsov[8]

[1]Fersman Mineralogical Museum of the Russian Academy of Sciences, Leninsky Prospekt 18-2, 119071 Moscow, Russia;

[2]Faculty of Geology, Moscow State University, Vorobievy Gory, 119991 Moscow, Russia;

[3]Department of Geological Sciences, Faculty of Science, Masaryk University, Kotlářská 2, 611 37 Brno, Czech Republic;

[4]Institute of Earth Sciences, St. Petersburg State University, University Emb. 7/9, 199034 Saint-Petersburg, Russia;

[5]Dipartimento di Geoscienze, Università di Padova, Via Gradenigo 6, I-35131, Padova, Italy;

[6]Dipartimento di Scienze della Terra, Università di Pisa, Via Santa Maria 53, I-56126 Pisa, Italy;

[7]Institute of Physics ASCR, v.v.i., Na Slovance 2, Prague 8, 18221, Czech Republic;

[8]Oktyabrskaya str., 5-337, 454071 Chelyabinsk, Russia

*Author for correspondence: Radek Škoda, E-mail: rskoda@sci.muni.cz

Abstract

The new mineral boevskite $Pb_4(TeO_3)_2(SO_4)(S_2O_3)$ was found at the Boevskoe W-Be deposit, Chelyabinsk Oblast, Southern Urals, Russia. It occurs as very rare euhedral grains up to 0.25 mm at the contact of galena and pyrite, as inclusions in galena up to 0.2 mm, and as thin veinlets up to 0.2 × 0.03 mm filling cracks in sphalerite. Other associated minerals include anglesite, cerussite, chalcopyrite, empressite, hessite, ingodite, joséite-B, matildite and pyrrhotite. Boevskite is colourless and transparent with an adamantine lustre. It is brittle, with uneven fracture. No cleavage or parting are observed. The Vickers' micro-indentation hardness (VHN, 10 g load) is 110 kg/mm^2, corresponding to a Mohs' hardness of 2.5–3. $D_{calc.}$ = 6.599 g/cm^3. Boevskite is optically biaxial, colourless and nonpleochroic. The mean refractive index calculated using the Gladstone-Dale equation is 2.08. The empirical formula

calculated on the basis of 13 O *apfu* is $Pb_{4.01}Te^{4+}_{2.03}S^{6+}_{1.97}S^{2-}_{0.98}O_{13}$. Boevskite is orthorhombic, space group *Pnma*, with a = 9.7764(7), b = 13.3622(10), c = 10.7213(9) Å, V = 1400.57(19) Å^3 and Z = 4. The strongest lines of the powder X-ray diffraction pattern [d, Å (I, %) (*hkl*)] are: 6.683 (65) (0 2 0), 3.355 (44) (1 0 3), 3.344 (52) (0 4 0), 3.289 (60) (2 3 0), 3.230 (100) (1 3 2), 3.144 (92) (2 3 1), 3.120 (51) (3 0 1), 2.787 (50) (0 3 3). The crystal structure of boevskite was refined from single-crystal X-ray diffraction data to R_1 = 0.0491 for 1538 reflections with $I > 2\sigma(I)$. Boevskite has a unique structure formed by Te–Pb–O layers coplanar to the *ac* plane with thiosulfate groups and SO_4 tetrahedra located between them. This is the first mineral having both sulfate and thiosulfate groups as species-defining constituents. It is named after the type locality.

Keywords: boevskite; new mineral; chemical composition; crystal structure; Raman spectroscopy; sulfate and thiosulfate groups; supergene mineralization; Boevskoe deposit; Southern Urals; Russia

Introduction

In recent years, the mineralogy and geochemistry of tellurium have attracted increasing attention from experts (Christy *et al.*, 2016; Krivovichev *et al.*, 2020; Missen *et al.*, 2020). A number of new tellurium oxysalts were described as a result of the discovery of new Te mineral localities (*e.g.*, Otto Mountain, Blue Bell Mine and Noth Star Mine in the USA, Ozernovskoe and Khokhoy Deposits in Russia, etc.) and investigation of new material from well-known Te deposits (Moctezuma Mine in Mexico, Tambo Mine in Chile etc.). In the course of the study by scanning electron microscopy with energy-dispersive spectrometry (SEM-EDS) of the fragments of quartz-sulfide veins from the abandoned Boevskoe (Russian Cyrillic – Боевское) W-Be deposit, Southern Urals, Russia, we encountered a supergene mineral phase having essential Pb, Te, S and O and a stoichiometry differing from all the already existing minerals with the same species-defining elements such as adanite, $Pb_2(Te^{4+}O_3)(SO_4)$ (Kampf *et al.*, 2020a), fairbankite, $Pb^{2+}_{12}(Te^{4+}O_3)_{11}(SO_4)$ (Missen *et al.*, 2021), northstarite, $Pb_6(Te^{4+}O_3)_5(S^{6+}O_3S^{2-})$ (Kampf *et al.*, 2020b) and schieffelinite, $Pb_{10}Te_6^{6+}O_{20}(OH)_{14}(SO_4)(H_2O)_5$ (Williams, 1980; Kampf *et al.*, 2012). Subsequent investigations of its crystal structure in combination with Raman and wavelength-dispersive spectroscopies showed this phase to be a new anhydrous lead tellurite sulfate thiosulfate. The simultaneous presence of both sulfate and thiosulfate groups as species-defining constituents is remarkable and recorded for the first time in a mineral. It was named boevskite [pronounced: bo ə vskait; Russian Cyrillic – боевскит] after the type locality. The new

https://doi.org/10.1180/mgm.2025.10143 Published online by Cambridge University Press

mineral, its name and symbol (Boe) have been approved by the Commission on New Minerals, Nomenclature and Classification of the International Mineralogical Association (CNMNC-IMA) (IMA2024–041, Kasatkin *et al.*, 2024). The holotype specimen is deposited in the systematic collection of the Fersman Mineralogical Museum of the Russian Academy of Sciences, Moscow with the catalogue number 98802.

Occurrence and general appearance

The new mineral occurs at the Boevskoe W-Be deposit, 35 km SW of the city of Kamensk-Uralskiy, Kaslinskiy District, Chelyabinsk Oblast, Southern Urals, Russia (56°14'44" N, 61°22'26" E; WGS84) (Fig. 1a).

The Boevskoe deposit has been mined for tungsten since the end of 19th century. It is known as the first tungsten deposit in Russia. For instance, during the second World War more than 80 tons of tungsten concentrate were mined. In the end of the 1940s, due to the low tungsten content in the ores compared to other deposits discovered at that time, the Boevskoe deposit was classified as a small-scale mining site and abandoned. In 1957, prospecting workings resumed and led to the discovery of beryl-fluorite-muscovite greisens with beryllium mineralization. The deposit was evaluated as large for beryllium reserves but poor for average beryllium content (0.12% BeO). Consequently, the industrial mining of beryllium ore never started. Currently, the deposit consists of numerous forested ditches up to several meters deep and collapsed adits (Figs 2a,b).

Geologically, the deposit is confined to the main fault that controls the location of the Boyevsko-Biktimirovskaya ore zone and comprises three tectonic blocks: western, eastern and central. In the western block, amphibolites are predominantly developed over pyroxene-plagioclase porphyrites and their tuffs (Fig. 1b). The eastern block is composed of carbonaceous, carbonaceous-micaceous schists and metamorphosed tuffaceous rocks. The central block is composed of biotite-albite and amphibole-biotite-albite schists, which are the result of metamorphism of the Middle Devonian volcanic-sedimentary and carbonate-terrigenous sedimentary rocks. The latter contain a subvolcanic body of metamorphosed gabbro, where quartz veins with wolframite (hübnerite) are confined. The central block includes two tectonic zones, western and eastern, each with a thickness of 200–300 m. The zones are sheet-like, consist of mylonites, and control fluorite-beryl metasomatic mineralization. Quartz-hübnerite veins have a sublatitudinal strike (70–80°) and dip to the south at angles of 60–90°. Main minerals of the veins are quartz, muscovite, fluorite, beryl, hübnerite and pyrite. Subordinate minerals include phenakite, fluorapatite, microcline, albite, calcite, scheelite, galena, sphalerite, pyrrhotite, rutile and supergene stolzite. The presence of

https://doi.org/10.1180/mgm.2025.10143 Published online by Cambridge University Press

sulfides in the ores of the deposit along with fluorite led to the formation of sulfuric and hydrofluoric acids in the oxidation zone and the active development of supergene processes to a depth of 100 meters (Rundqvist and Chistyakov, 1960; Zabolotnaya, 1978; Zoloev *et al*., 2004; Kupriyanova and Shpanov, 2011; Ponomarev *et al*., 2022).

The samples containing the new mineral were collected in May and July 2023 on the border of an old collapsed adit used for tungsten mining in the first half of 20th century (Fig. 2b). Macroscopically, the samples are represented by fragments of a quartz vein with visible galena, pyrite, sphalerite and muscovite. Boevskite was discovered during SEM-EDS analysis of polished sections prepared from these samples. The new mineral occurs as very rare idiomorphic grains up to 0.25 mm developed at the contact of galena and pyrite (Fig. 3a), as inclusions in galena up to 0.2 mm, or as thin veinlets up to 0.2 × 0.03 mm filling cracks in sphalerite (Fig. 3b). Some grains are rimmed by later anglesite. Apart from the minerals mentioned above, boevskite is associated with cerussite and primary chalcopyrite, matildite, pyrrhotite and several tellurides (empressite, hessite, ingodite, joséite-B). The latter occur in the same rock but not in the direct contact with boevskite.

The new mineral was formed as a result of the supergene alteration of the co-existing galena and tellurides (empressite, hessite, ingodite, joséite-B) in the oxidation zone.

The Boevskoe deposit is the type locality of glucine, $CaBe_4(PO_4)_2(OH)_4 \cdot 0.5H_2O$ (Grigoriev, 1963) and uralolite, $Ca_2Be_4(PO_4)_3(OH)_3 \cdot 5H_2O$ (Grigoriev, 1964). Thus, boevskite is the third new mineral discovered here.

Physical properties and optical data

Boevskite is colourless and transparent with a white streak and adamantine lustre. It is brittle, with uneven fracture. No cleavage and parting are observed. It does not fluoresce under ultraviolet light. The Vickers' micro-indentation hardness (VHN, 10 g load) is 110 kg/mm^2 (range 97–124, n = 3), corresponding to a Mohs' hardness of 2.5–3. The density of the mineral could not be measured due to the very small amount of available material and absence of heavy liquids with suitable density. A density value calculated using the empirical formula and unit-cell volume obtained from single-crystal X-ray diffraction (SCXRD) data is 6.599 g/cm^3. Boevskite is biaxial, colourless and non-pleochroic in transmitted plane-polarized light. Its refractive indices (RI) could not be measured because of the absence of immersion liquids that can measure RI values higher than 2.0. The Gladstone-Dale relationship (Mandarino, 1981) predicts an average index of refraction of 2.08 which is comparable to the value of 2.15 calculated for northstarite, $Pb_6(Te^{4+}O_3)_5(S^{6+}O_3S^{2-})$, the only other thiosulfate-tellurite of Pb (Kampf *et al*., 2020b). Optical properties of boevskite were

https://doi.org/10.1180/mgm.2025.10143 Published online by Cambridge University Press

therefore studied using the methods common for opaque minerals. In reflected light, boevskite is grey, a little lighter than neighbouring anglesite but little darker than sphalerite and much darker than galena and especially pyrite. No visible bireflectance and pleochroism are observed. In crossed polars it is weakly anisotropic, in grey tones. Internal reflections were not observed. The set of reflectance measurements performed in air relative to a Si standard by means of an MSF-R (LOMO, St. Petersburg, Russia) microspectrophotometer is given in Table 1.

Raman Spectroscopy

The Raman spectrum of boevskite was obtained by means of a Horiba Labram HR Evolution spectrometer. This dispersive, edge-filter-based system is equipped with an Olympus BX 41 optical microscope, a diffraction grating with 600 grooves per millimetre, and a Peltier-cooled, Si-based charge-coupled device (CCD) detector. The Raman data were collected using a 532 nm laser. The nominal laser beam energy of 50 mW was attenuated to 25% using a neutral density filter to avoid the thermal damage of the analysed area. Raman signal was collected in the range of 50–4000 cm^{-1} with a 50× objective and the system being operated in confocal mode with a beam diameter of ~2.6 μm and an axial resolution of ~5 μm. Time acquisition was 60 s per spectral window; 5 accumulations and 7 spectral windows were applied to cover the 50–4000 cm^{-1} range. Wavenumber calibration was done using the Rayleigh line and low-pressure Ne-lamp emissions. The wavenumber accuracy was ~0.5 cm^{-1}, and the spectral resolution was ~2 cm^{-1}. Band fitting was done after appropriate background correction, assuming combined Lorentzian-Gaussian band shapes using a Voigt function (*PeakFit*; Jandel Scientific Software). As there were no Raman bands observed in the region above 1200 cm^{-1}, the Raman spectrum is shown in the range 50–1250 cm^{-1} (Fig. 4).

Raman bands of boevskite were assigned according to the systematic study of synthetic thiosulfates (Gabelica, 1980) and sulfate and tellurite phases (Buzgar *et al*., 2009; Frost *et al*., 2009).

Raman scattering in the range 950–1150 cm^{-1} correspond to stretching vibrations of the SO_4 and S_2O_3 tetrahedra. The more intense bands at 954 and 976 cm^{-1} correspond to symmetric stretching, whereas the less intense bands at 1047, 1096 and 1133 cm^{-1} are interpreted as antisymmetric stretching of the SO_4 and S_2O_3 groups. The spectrum of boevskite is dominated by a strong band at 741 cm^{-1} corresponding to the symmetric stretching vibrations of TeO_3 groups. The less intense Raman bands in the region 550–700

https://doi.org/10.1180/mgm.2025.10143 Published online by Cambridge University Press

cm^{-1} represent bending modes of SO_4 and S_2O_3 groups overlapping with antisymmetric stretching vibrations of TeO_3 groups. The isolated weak Raman band at 521 cm^{-1} is attributed to a thiosulfate bending mode. Raman bands in the region 300–500 cm^{-1} are dominated by a sharp, intense band at 445 cm^{-1} corresponding to vibration of the S–S bond. Additionally, rotation modes of the SO_4 and S_2O_3 groups overlapping with symmetrical bending modes of SO_4 and S_2O_3 groups and bending modes of TeO_3 groups are present. The Raman bands < 300 cm^{-1} are attributed to Pb–O vibrations and lattice modes.

Chemical Data

Quantitative chemical analyses were carried out using a Cameca SX 100 electron microprobe (WDS mode, 15 kV, 10 nA, 3 μm beam diameter) at the Department of Geological Sciences, Faculty of Science, Masaryk University, Brno, Czech Republic. The structure determination and Raman spectrum indicate boevskite to contain one sulfate and one thiosulfate group, so the measured content of SO_3 was allocated as SO_3 and S based upon S^{6+}:S^{2-} = 2:1. The crystal structure and Raman spectroscopy data also confirm the absence of H_2O, OH groups, as well as B–O, C–O and N–O bonds in the mineral. Contents of other elements with atomic numbers higher than that of C other than Pb, Te, S, and O are below detection limits. Raw X-ray intensities were corrected for matrix interactions using the X-PHI algorithm (Merlet, 1994). Analytical data and the list of standards are given in Table 2.

The empirical formula calculated on the basis of 13 O atoms per formula unit is $Pb_{4.01}Te^{4+}_{2.03}S^{6+}_{1.97}S^{2-}_{0.98}O_{13}$. The ideal formula of boevskite is $Pb_4(TeO_3)_2(SO_4)(S_2O_3)$, which requires PbO 64.31, TeO_2 23.00, SO_3 11.53, S 2.31, O=S –1.15, total 100 wt.%.

Boevskite slowly dissolves in concentrated hydrochloric acid.

X-ray Crystallography

Due to the lack of material, powder X-ray diffraction (PXRD) data were collected from the same grain used for SCXRD studies, using a Rigaku R-AXIS Rapid II single-crystal diffractometer equipped with a cylindrical image plate detector (radius 127.4 mm) using Debye-Scherrer geometry, Co*K*α radiation (rotating anode with VariMAX microfocus optics), 40 kV and 15 mA. The angular resolution of the detector is 0.045° 2θ (pixel size 0.1 mm). The data were integrated using the software package *Osc2Tab* (Britvin *et al.*, 2017). PXRD data for boevskite are given in Table 3 in comparison to that calculated from SCXRD data using the *Atoms 5.1* program (Dowty, 2000). It should be noted that preferential orientation of the single crystal during PXRD data collection introduces some minor differences in the intensity of peaks in the observed and calculated powder diffraction patterns, while maintaining their angular positions. Parameters of an orthorhombic unit-cell

https://doi.org/10.1180/mgm.2025.10143 Published online by Cambridge University Press

were calculated from the observed *d* spacing data using *UnitCell* software (Holland and Redfern, 1997) and are as follows: a = 9.774(3), b = 13.364(3), c = 10.716(3) Å, and V = 1399.7(8) Å^3.

For the SCXRD study, a grain of boevskite, 0.031 × 0.035 × 0.041 mm^3 in size, extracted from the polished section analysed using electron microprobe and Raman spectroscopy, was mounted on a glass fiber and examined with a Rigaku Oxford Diffraction XtaLAB Synergy-S single-crystal X-ray diffractometer (monochromated microfocused Mo*K*α radiation, λ = 0.71073 Å; 50 kV, 1 mA) equipped with an area hybrid photon-counting HyPix-6000HE detector. The data were collected by 376 frames over 5 runs; the exposure time was 170 seconds per frame. The data were processed by *CrysAlisPro* 1.171.42.49 software (Rigaku Oxford Diffraction, 2022) and are as follows: boevskite is orthorhombic, space group *Pnma*, with unit-cell parameters a = 9.7764(7), b = 13.3622(10), c = 10.7213(9) Å, V = 1400.57(19) Å^3 and Z = 4.

The crystal structure of boevskite was solved by direct methods and refined to R_1 = 0.0491 for 1538 reflections with $I > 2\sigma(I)$ using SHELXS and SHELXL software package (Sheldrick, 2008; 2015). Crystal data, data collection information and structure refinement details for boevskite are given in Table 4. Coordinates and displacement parameters of atoms are given in Table 5 and selected interatomic distances in Table 6. The crystallographic information file has been deposited in the Inorganic Crystal Structure Database (ICSD) and can be obtained by quoting the CSD 2440705 *via* www.ccdc.cam.ac.uk/structures/, and also is available as Supplementary material (see below).

Description of Crystal Structure

The crystal structure of boevskite is unique (Fig. 5). It contains two non-equivalent Pb^{2+} sites and one Te^{4+} site, which are characterized by off-center coordinations that are typical for cations with lone-pair electrons (Christy and Mills, 2013). The Pb1 cation has four relatively short Pb1–O bonds in the range 2.34–2.60 Å, three longer Pb1–O bonds (2.79-2.95 Å), and one significantly elongated Pb1–S3 bond (3.49 Å) to S^{2-}. The Pb2 site is coordinated by nine O^{2-} anions with four relatively short Pb2–O bonds in the range 2.56–2.73 Å, five longer Pb2–O bonds in the range 2.86–3.31 Å, and one bond to S^{2-} (3.03 Å). The Te site is coordinated by O^{2-} anions with three short Te–O bonds (<1.93 Å) on one side of Te site, thus defining the $Te^{4+}O_3$ pyramid with the Te cation as its apical vertex, which is the most common coordination for Te^{4+} in oxysalts (Christy *et al.*, 2016). The Te cation is also coordinated by

https://doi.org/10.1180/mgm.2025.10143 Published online by Cambridge University Press

five O atoms with significantly elongated Te–O distances (2.66–3.30 Å) on the opposite side from the short Te–O bonds (Table 6).

There are three crystallographically non-equivalent S sites in the structure of boevskite. The S1 site is tetrahedrally coordinated by O atoms whereas S2 and S3 participate in the formation of a thiosulfate group $S_2O_3^{2-}$ or $(S2^{6+}O_3S3^{2-})^{2-}$. S–O distances in the SO_4 tetrahedron and in the thiosulfate group as well as S^{6+}–S^{2-} distance in thiosulfate tetrahedron are in good agreement with the corresponding distance ranges reported for sulfate and thiosulfate tetrahedra (Hawthorne *et al.*, 2000). Considering the short Te–O and relatively short Pb–O bonds, the structure of boevskite can be described as formed by Te–Pb–O layers coplanar to the *ac* plane with thiosulfate groups and SO_4 tetrahedra located between them and only weakly linked to the layers. It is noteworthy that rather rigid structural units like TeO_3 pyramids, SO_4 tetrahedra and thiosulfate ($S^{6+}O_3S^{2-}$) groups are isolated one from another.

Discussion

Boevskite has no structural analogues or relatives among minerals. In general, minerals with the simultaneous presence of different species-defining S–O groups are extremely rare. Up-to-date, only three sulfate-sulfites are known: orschallite $Ca_3(SO_3)_2(SO_4)\cdot 12H_2O$ (Weidenthaler *et al.*, 1993), hielscherite $Ca_3Si(OH)_6(SO_4)(SO_3)\cdot 11H_2O$ (Pekov *et al.*, 2012) and tomiolloite $Al_{12}(Te^{4+}O_3)_5[(SO_3)_{0.5}(SO_4)_{0.5}](OH)_{24}$ (Missen *et al.*, 2022). Moreover, similarly to boevskite, the latter is also a tellurite. However, boevskite is the first mineral containing both sulfate and thiosulfate groups as species-defining constituents at distinct structural positions. During the preparation of this article, another sulfate-thiosulfate has been approved by CNMNC-IMA – blueridgeite $[Pb_8Zn_3Cu^{2+}(OH)_{16}](SO_4)_2(S_2O_3)_2\cdot 2H_2O$ from Redmond Mine, North Carolina, USA (Emproto *et al.*, 2025). The substitution of a small amount of thiosulfate for sulfate and *vice versa* have been reported earlier in several new lead sulfate and thiosulfate minerals from the above-mentioned mine in North Carolina, such as sulfatoredmondite $[Pb_8O_2Zn(OH)_6](SO_4)_4\cdot 6H_2O$ (Kampf *et al.*, 2023a), cubothioplumbite and hexathioplumbite, dimorphs with the formula $[Pb_4OH_4]Pb(S_2O_3)_3$ (Kampf *et al.*, 2023b), cherokeeite $[Pb_2Zn(OH)_4](SO_4)\cdot H_2O$ and cuprocherokeeite $[Pb_8Zn_3Cu^{2+}(OH)_{16}](SO_4)_4\cdot 4H_2O$ (Kampf *et al.*, 2023c), finescreekite $[Pb_4(OH)_4](S_2O_3)_2$ and hayelasdiite $[Pb_4O_{1.5}(OH)_{2.5}]_2[Cu^{+}{}_5(S_2O_3)_4(S_2O_2OH)_2(H_2O)]\cdot 4H_2O$ (Kampf *et al.*, 2024a), boojumite $Pb_8O_4(OH)_2(S_2O_3)_3$ and kennygayite $[Pb_4O_2(OH)_2](SO_4)$ (Kampf *et al.*, 2024b). The mineral chemically closest to boevskite is northstarite, a lead-tellurite-thiosulfate with the formula $Pb_6(Te^{4+}O_3)_5(S_2O_3)$ (Kampf *et al.*, 2020b). However, it does not contain sulfate groups, and its structure is completely different. Some structural similarity in the topology of Te–Pb–O

https://doi.org/10.1180/mgm.2025.10143 Published online by Cambridge University Press

layers in boevskite could be found with the layers in the structure of another chemically similar mineral, adanite $Pb_2(Te^{4+}O_3)(SO_4)$, where the most rigid structural units are TeO_3 pyramids and SO_4 tetrahedra, while the strongest bonds between structural units are similarly the short bonds between the Pb^{2+} cations and O atoms of the $Te^{4+}O_3$ pyramids (Kampf *et al*., 2020a). Taking into account short Pb–O (the fourth elongated Pb2–O bond of 2.77 Å in the structure of adanite should also be considered for better comparison) and Te–O bonds in both minerals, the topological similarity of their layers is shown in Fig. 6. The other two minerals having same species-defining elements as boevskite, *i.e.* fairbankite, $Pb^{2+}{}_{12}(Te^{4+}O_3)_{11}(SO_4)$ (Missen *et al.*, 2021) and schieffelinite, $Pb_{10}Te_6{}^{6+}O_{20}(OH)_{14}(SO_4)(H_2O)_5$ (Williams, 1980; Kampf *et al*., 2012) are characterized by a structure topology strongly differing from that of boevskite. They do not contain thiosulfate groups and schieffelinite, moreover, is a tellurate and not tellurite.

Boevskite was formed proximally as a result of the oxidative decomposition of primary sulfides and tellurides. The oxidation of pyrite and galena under neutral to alkaline conditions (pH > 7) releases thiosulfate and sulfate oxoanions, with sulfate concentrations decreasing as pH increases up to ~ pH 9 (Gardner and Woods, 1979; Goldhaber, 1983). Therefore, boevskite likely forms in this pH range. Moreover, alkaline conditions inhibit the formation of anglesite (Keim and Markl, 2015), and low dissolved carbonate concentrations prevent the formation of cerussite. Neutral to alkaline conditions were also considered by Bindi *et al.* (2011) for the crystallization of another thiosulfate mineral, fassinaite $Pb_2{}^{2+}(S_2O_3)(CO_3)$, described from the Trentini mine, Mount Naro, Italy and the Erasmus adit, Schwarzleo District, Austria. Subsequent overgrowing of boevskite by anglesite probably reflects mineral-forming solution evolution to lower pH values. Consequently, the proximal or distal formation of boevskite in other ore deposits could be expected if similar geochemical conditions were present during the alteration of mineral associations containing primary Pb sulfides or sulfosalts and Te minerals.

Supplementary material

To view supplementary material for this article, please visit: https://doi.org/...

Acknowledgements

We thank Associate Editor Anthony Kampf, Reviewer Igor V. Pekov and two anonymous reviewers for constructive comments that improved the manuscript. Maria D. Milshina and Ekaterina V. Vorontsova are acknowledged for the help with the figures. This work in part of structural and crystal chemical analysis was supported by the Russian Science

https://doi.org/10.1180/mgm.2025.10143 Published online by Cambridge University Press

Foundation [grant No. 25-17-00005] (for N.V.Z.). The PXRD studies have been performed at the Research Centre for X-ray Diffraction Studies of St. Petersburg State University within the framework of the project 125021702335-5.

References

Bindi L., Nestola F., Kolitsch U., Guastoni A. and Zorzi F. (2011) Fassinaite, $Pb_2^{2+}(S_2O_3)(CO_3)$, the first mineral with coexisting thiosulphate and carbonate groups: description and crystal structure. *Mineralogical Magazine*, **75**, 2721–2732.

Brese N.E. and O'Keeffe M. (1991) Bond-valence parameters for solids. *Acta Crystallographica*, **47**, 192–197.

Britvin S.N., Dolivo-Dobrovolsky D.V. and Krzhizhanovskaya M.G. (2017) Software for processing the X-ray powder diffraction data obtained from the curved image plate detector of Rigaku RAXIS Rapid II diffractometer. *Zapiski Rossiiskogo Mineralogicheskogo Obshchestva*, **146**, 104–107 (in Russian).

Buzgar N., Buzatu A. and Sanislav I.V. (2009) The Raman study on certain sulfates. *Annals of the "Alexandru Ioan Cuza" University of Iaşi. Geologie*, **55**(1), 5–23.

Christy A.G. and Mills S.J. (2013) Effect of lone-pair stereoactivity on polyhedral volume and structural flexibility: Application to $Te^{IV}O_6$ octahedra. *Acta Crystallographica*, **B69**, 446–456.

Christy A.G., Mills S.J. and Kampf A.R. (2016) A review of the structural architecture of tellurium oxycompounds. *Mineralogical Magazine*, **80**, 415–545.

Dowty E. (2000) ATOMS - Atomic Structure Display. Version 5.1. Kingsport, IN, USA.

Emproto C., Olds T.A., Kampf A.R., Smith J.B., Hughes J.M. and Ma C. (2025) Blueridgeite, IMA 2024-071. CNMNC Newsletter 84, European Journal of Mineralogy, **37**, https://doi.org/10.5194/ejm-37-249-2025.

Frost R.L., Čejka J. and Dickfos M.J. (2009) Raman spectroscopic study of the uranyl tellurite mineral moctezumite $PbUO_2(TeO_3)_2$. *Journal of Raman Spectroscopy: An International Journal for Original Work in all Aspects of Raman Spectroscopy, Including Higher Order Processes, and also Brillouin and Rayleigh Scattering*, **40**(1), 38–41.

Gardner J.R. and Woods R. (1979) A study of the surface oxidation of galena using cyclic voltammetry. *Journal of Electroanalytical Chemistry and Interfacial Electrochemistry*, **100**, 447–459.

Gagné O.C. and Hawthorne F.C. (2015) Comprehensive derivation of bond-valence parameters for ion pairs involving oxygen. *Acta Crystallographica*, B**71**, 562–578.

https://doi.org/10.1180/mgm.2025.10143 Published online by Cambridge University Press

Gabelica Z. (1980) Structural study of solid inorganic thiosulfates by infrared and Raman spectroscopy. *Journal of Molecular Structure*, **60**, 131–138.

Goldhaber M.B. (1983) Experimental study of metastable sulfur oxyanion formation during pyrite oxidation at pH 6-9 and 30 degrees C. *American Journal of Science*, **283**, 193–217.

Grigoriev N.A. (1963) Glucine – a new beryllium mineral. *Zapiski Vsesoyuznogo Mineralogicheskogo Obshchestva*, **92**, 691–696 (in Russian).

Grigoriev N.A. (1964) Uralolite – a new mineral. *Zapiski Vsesoyuznogo Mineralogicheskogo Obshchestva*, **93**, 156–162 (in Russian).

Hawthorne F.C., Krivovichev S.V. and Burns P.C. (2000) The crystal chemistry of sulfate minerals. *Reviews in Mineralogy and Geochemistry*, **40**, 1–112.

Holland T.J.B. and Redfern S.A.T. (1997) Unit cell refinement from powder diffraction data: the use of regression diagnostics. *Mineralogical Magazine*, **61**, 65–77.

Kampf A.R., Mills S.J., Housley R.M., Rumsey M.S. and Spratt J. (2012) Lead-tellurium oxysalts from Otto Mountain near Baker, California: VII. Chromschieffelinite, $Pb_{10}Te_6O_{20}(OH)_{14}(CrO_4)(H_2O)_5$, the chromate analog of schieffelinite. *American Mineralogist*, **97**, 212–219.

Kampf A.R., Housley R.M., Rossman G.R., Yang H. and Downs R.T. (2020a) Adanite, a new lead-tellurite-sulfate mineral from the North Star mine, Tintic, Utah, and Tombstone, Arizona, U.S.A. *The Canadian Mineralogist*, **58**, 403–410.

Kampf A.R., Housley R.M. and Rossman G.R. (2020b) Northstarite, a new lead-tellurite-thiosulfate mineral from the North Star mine, Tintic, Utah, USA. *The Canadian Mineralogist*, **58**, 533–542.

Kampf A.R., Smith J.B., Hughes J.M., Ma C. and Emproto C. (2023a) New minerals from the Redmond mine, North Carolina, USA: I. Redmondite, hydroredmondite, and sulfatoredmondite, three minerals containing the novel $[Pb_8O_2Zn(OH)_6]^{8+}$ structural unit. *The Canadian Journal of Mineralogy and Petrology*, **61**, 189–202.

Kampf A.R., Smith J.B., Hughes J.M., Ma C. and Emproto C. (2023b) New minerals from the Redmond mine, North Carolina, USA: II. Cubothioplumbite and hexathioplumbite, two new minerals containing the cubane-like $[Pb_4(OH)_4]^{4+}$ structural unit. *The Canadian Journal of Mineralogy and Petrology*, **61**, 623–633.

Kampf A.R., Smith J.B., Hughes J.M., Ma C. and Emproto C. (2023c) New minerals from the Redmond mine, North Carolina, USA: III. Cherokeeite and cuprocherokeeite, two

https://doi.org/10.1180/mgm.2025.10143 Published online by Cambridge University Press

new minerals containing $[Pb_2(Zn,Cu^{2+})(OH)_4]^{2+}$ chains. *The Canadian Journal of Mineralogy and Petrology*, **61**, 635–647.

Kampf A.R., Smith J.B., Hughes J.M., Ma C. and Emproto C. (2024a) New minerals from the Redmond mine, North Carolina, USA: V. Finescreekite and hayelasdiite, two new thiosulfate minerals containing cubane-like Pb_4O_4 structural units. *The Canadian Journal of Mineralogy and Petrology*, **62**, 379–390.

Kampf A.R., Smith J.B., Hughes J.M., Ma C. and Emproto C. (2024b) New minerals from the Redmond mine, North Carolina, USA: VI. Boojumite and kennygayite, two new minerals with structures based on chains of oxocentered OPb_4 tetrahedra. *The Canadian Journal of Mineralogy and Petrology*, **62**, 391–403.

Kasatkin A.V., Zubkova N.V., Škoda R., Gurzhiy V.V., Nestola F., Biagioni C., Agakhanov A.A., Britvin S.N., Plašil J. and Kuznetsov A.M. (2024) Boevskite, IMA 2024-041. CNMNC Newsletter 81, *Mineralogical Magazine*, **88**, https://doi.org/10.1180/mgm.2024.77.

Keim M.F. and Markl G. (2015) Weathering of galena: Mineralogical processes, hydrogeochemical fluid path modeling, and estimation of the growth rate of pyromorphite. *American Mineralogist*, **100**, 1584–1594.

Krivovichev V.G., Krivovichev S.V. and Charykova M.V. (2020) Tellurium Minerals: Structural and Chemical Diversity and Complexity. *Minerals*, **10,** 623.

Kupriyanova I.I. and Shpanov E.P. (2011) Beryllium deposits of Russia. Moscow, "GEOS", 353 p. (in Russian).

Mandarino J.A. (1981) The Gladstone-Dale relationship: Part IV. The compatibility concept and its application. *The Canadian Mineralogist*, **19**, 441–450.

Merlet C. 1994: An Accurate Computer Correction Program for Quantitative Electron Probe Microanalysis. *Microchimica Acta*, **114/115**, 363–376.

Mills S.J. and Christy A.G. (2013) Revised values of the bond-valence parameters for Te^{IV}-O, Te^{VI}-O and Te^{IV}-Cl. *Acta Crystallographica*, **B69**, 145–149.

Missen O.P., Ram R., Mills S.J., Etschmann B., Reith F., Shuster J., Smith D.J. and Brugger J. (2020) Love is in the Earth: A review of tellurium (bio)geochemistry in surface environments. *Earth-Science Reviews*, **204**, 103150.

Missen O.P., Rumsey M.S., Mills S.J., Weil M., Najorka J., Spratt J. and Kolitsch U. (2021) Elucidating the natural–synthetic mismatch of $Pb^{2+}Te^{4+}O_3$: The redefinition of fairbankite to $Pb^{2+}_{12}(Te^{4+}O_3)_{11}(SO_4)$. *American Mineralogist*, **106**, 309–316.

https://doi.org/10.1180/mgm.2025.10143 Published online by Cambridge University Press

Missen O.P., Mills S.J., Rumsey M.S., Spratt J., Najorka J., Kampf A.R. and Thorne B. (2022) The new mineral tomiolloite, $Al_{12}(Te^{4+}O_3)_5[(SO_3)_{0.5}(SO_4)_{0.5}](OH)_{24}$: A unique microporous tellurite structure. *American Mineralogist*, **107**, 2167–2175.

Pekov I.V., Chukanov N.V., Britvin S.N., Kabalov Y.K., Göttlicher J., Yapaskurt V.O., Zadov A.E., Krivovichev S.V., Schüller W. and Ternes B. (2012) The sulfite anion in ettringite-group minerals: a new mineral species hielscherite, $Ca_3Si(OH)_6(SO_4)(SO_3)\cdot 11H_2O$, and the thaumasite-hielscherite solid-solution series. *Mineralogical Magazine*, **76**, 1133–1152.

Ponomarev V.S., Erokhin, Yu.V. and Grigoriev V.V. (2022) On the mineralogy of the Boevskoe tungsten deposit: new data. *Bulletin of the Ural Branch of the Russian Mineralogical Society*, **19**, 108–114 (in Russian).

Rigaku Oxford Diffraction, *CrysAlisPro Software system, version 1.171.42.49*, 2022.

Rundqvist D.V. and Chistyakov N.E. (1960) On the beryl-fluorite-muscovite type of mineralization. *Geology of Ore Deposits*, **2**, 44–52 (in Russian).

Sheldrick G.M. (2008) A short history of SHELX. *Acta Crystallographica*, **A64**, 112–122.

Sheldrick G.M. (2015) Crystal structure refinement with SHELXL. *Acta Crystallographica*, **C71**, 3–8.

Weidenthaler C., Tillmanns E. and Hentschel G. (1993) Orschallite, $Ca_3(SO_3)_2(SO_4)\cdot 12H_2O$, a new calcium-sulfite-sulfate-hydrate mineral. *Mineralogy and Petrology*, **48**, 167–177.

Williams S.A. (1980) Schieffelinite, a new lead tellurate-sulphate from Tombstone, Arizona. *Mineralogical Magazine*, **43**, 771–773.

Zabolotnaya N.P. (1978) Muscovite-fluorite-beryl type of deposits. Pp. 364–367 in: Ore deposits of USSR. Volume 3. Moscow, “Nedra”, 496 p. (in Russian).

Zoloev K.K., Levin V.Ya., Mormil S.I. and Schardakova G.Yu. (2004) Minerageny and deposits of rare metals, molybdenum, tungsten of the Urals. Yekaterinburg, Ministry of Natural Resources of the Russian Federation, GUPR for the Sverdlovsk Region, Institute of Geology and Geochemistry named after A.N. Zavaritskiy UrO RAN, OAO UGSE, 336 p. (in Russian).

https://doi.org/10.1180/mgm.2025.10143 Published online by Cambridge University Press

Table 1. Reflectance values for boevskite (COM standard wavelengths are given in bold).

λ (nm)	R_{max} (%)	R_{min} (%)		λ (nm)	R_{max} (%)	R_{min} (%)
400	15.7	15.1		560	13.5	13.2
420	15.4	14.9		580	13.5	13.2
440	15.1	14.6		**589**	**13.5**	**13.2**
460	14.8	14.2		600	13.5	13.2
470	**14.7**	**14.1**		620	13.4	13.1
480	14.5	13.9		640	13.6	13.1
500	14.0	13.5		**650**	**13.8**	**13.2**
520	13.5	13.2		660	13.9	13.2
540	13.5	13.1		680	14.2	13.4
546	**13.5**	**13.1**		700	14.6	13.6

Table 2. Chemical composition (in wt%) of boevskite.

Constituent	**Average**	**Range**	**Stand. Dev.**	**Reference Material**
PbO	64.83	64.71–65.20	0.20	Anglesite
TeO_2	23.52	23.43–23.70	0.09	TeO_2
SO_3*	(17.16)	16.33–17.63	0.50	Baryte
SO_3**	11.44			
S**	2.29			
O=S	–1.14			
Total	**100.94**			

* Total measured value

** Calculated values based on the structure (S^{6+}:S^{2-} = 2:1).

Table 3. Powder X-ray diffraction data (*d* in Å) of boevskite.

d_{obs}	I_{obs}	d_{calc}*	I_{calc}**	*h k l*	d_{obs}	I_{obs}	d_{calc}*	I_{calc}**	*h k l*
6.683	**65**	**6.681**	**58**	**0 2 0**			2.279	16	3 4 1
		4.591	11	2 1 0			2.265	8	3 2 3
		4.434	25	1 1 2	2.225	27	2.227	18	0 6 0
		4.220	18	2 1 1			2.224	15	4 0 2
		3.945	7	2 2 0	2.186	12	2.183	12	2 4 3
		3.844	5	1 2 2			2.139	14	3 4 2
		3.612	13	2 0 2			2.117	6	0 1 5
3.488	26	3.487	21	2 1 2	2.100	12	2.101	9	4 3 1
3.451	27	3.452	17	0 1 3	2.049	5	2.046	10	3 1 4
3.355	**44**	**3.357**	**54**	**1 0 3**			2.044	6	1 4 4
3.344	**52**	**3.341**	**24**	**0 4 0**			1.964	8	2 0 5
3.289	**60**	**3.292**	**41**	**2 3 0**			1.932	10	0 3 5
		3.255	13	1 1 3	1.928	13	1.928	8	3 5 2
3.230	**100**	**3.233**	**84**	**1 3 2**			1.924	7	5 0 1
		3.177	6	2 2 2			1.904	6	5 1 1
3.144	**92**	**3.147**	**100**	**2 3 1**			1.877	19	3 3 4

https://doi.org/10.1180/mgm.2025.10143 Published online by Cambridge University Press

3.120	**51**	**3.118**	**37**	**3 0 1**			1.858	6	1 5 4
3.033	34	3.036	15	3 1 1			1.856	11	1 6 3
		3.021	17	1 4 1			1.812	6	3 6 1
2.996	28	2.999	15	1 2 3			1.806	7	4 0 4
		2.885	12	2 0 3			1.797	10	2 3 5
2.832	19	2.835	16	0 4 2	1.764	6	1.766	15	5 3 1
		2.825	6	3 2 1			1.758	6	1 0 6
		2.805	10	2 3 2			1.739	6	3 6 2
2.787	**50**	**2.787**	**31**	**0 3 3**			1.693	6	2 4 5
		2.785	25	3 0 2			1.688	7	2 7 2
2.677	32	2.681	22	1 3 3			1.684	5	0 7 3
		2.680	9	0 0 4			1.628	8	3 7 1
2.595	16	2.593	8	0 5 1			1.627	5	1 8 1
		2.554	18	3 3 1	1.613	20	1.610	5	5 4 2
		2.421	5	2 3 3			1.556	6	1 4 6
		2.408	5	3 0 3			1.489	6	5 3 4
2.327	7	2.323	12	1 5 2			1.246	9	4 3 7
		2.291	9	2 5 1			1.232	6	4 7 5

* For the calculated pattern, only reflections with intensities ≥5 are given.
** For the unit-cell parameters obtained from single crystal data.
Strongest reflections are given in boldtype.

Table 4. Single-crystal X-ray diffraction data collection information and structure refinement parameters for boevskite.

Formula	$Pb_4(TeO_3)_2(SO_4)(S_2O_3)$
Formula weight	1388.14
Temperature, K	293(2)
Radiation and wavelength, Å	Mo$K\alpha$; 0.71073
Crystal system, space group, Z	Orthorhombic, *Pnma*, 4
Unit cell dimensions, Å	a = 9.7764(7) b = 13.3622(10) c = 10.7213(9)
V, Å^3	1400.57(19)
Absorption coefficient μ, mm^{-1}	52.53
F_{000}	2336
Crystal size, mm^3	0.031 × 0.035 × 0.041
Diffractometer	Rigaku Oxford Diffraction XtaLAB Synergy-S
θ range for data collection, °	3.21 – 29.99
Index ranges	$-12 \le h \le 13$, $-18 \le k \le 17$, $-15 \le l \le 12$
Reflections collected	8506
Independent reflections	2088 (R_{int} = 0.0954)
Independent reflections with I>2σ(I)	1538

https://doi.org/10.1180/mgm.2025.10143 Published online by Cambridge University Press

Data reduction	*CrysAlisPro*, v. 1.171.42.49 (Rigaku OD, 2022)
Absorption correction	gaussian
Structure solution	direct methods
Refinement method	full-matrix least-squares on F^2
Number of refined parameters	109
Final R indices [$I>2\sigma(I)$]	R_1 = 0.0491, wR_2 = 0.1061
R indices (all data)	R_1 = 0.0725, wR_2 = 0.1156
GoF	0.984
Largest diff. peak and hole, e/Å^3	3.42 and -2.87

Table 5. Coordinates and displacement parameters (U_{eq}, Å^2) of atoms and bond valence sums (BVS) for boevskite calculated using the parameters taken from Gagné and Hawthorne (2015) for Pb–O and S–O, from Brese and O'Keeffe (1991) for Pb–S^{2-} and S^{6+}–S^{2-} and from Mills and Christy (2013) for Te–O.

Site	x	y	z	U_{eq}	BVS
Pb1	0.63071(5)	0.39103(4)	0.05132(5)	0.01894(16)	2.03
Pb2	0.48837(5)	0.56566(4)	0.33267(6)	0.02566(17)	1.84
Te	0.75432(8)	0.40147(6)	0.38251(8)	0.0155(2)	4.04
S1	0.9480(5)	0.25	0.1693(5)	0.0167(9)	5.91
S2	0.6701(5)	0.75	0.1595(5)	0.0206(10)	5.75
S3	0.6679(6)	0.75	0.3476(6)	0.0297(12)	1.86
O1	0.6883(9)	0.4671(7)	0.2404(10)	0.022(2)	2.10
O2	0.9217(9)	0.4732(8)	0.3861(9)	0.019(2)	2.08
O3	0.5989(11)	0.6607(8)	0.1157(11)	0.031(3)	1.90
O4	0.9958(14)	0.25	0.2986(15)	0.027(3)	1.96
O5	0.6667(10)	0.4934(7)	0.4885(9)	0.020(2)	2.08
O6	0.7954(13)	0.25	0.1712(14)	0.022(3)	1.93
O7	0.9959(12)	0.1590(10)	0.1040(13)	0.038(3)	1.82
O8	0.8136(15)	0.75	0.1175(17)	0.037(4)	1.77

https://doi.org/10.1180/mgm.2025.10143 Published online by Cambridge University Press

Table 6. Selected interatomic distances (Å) in the structure of boevskite.

Pb1 – O1 2.337(10)	Te – O1 1.872(10)
– O2 2.414(9)	– O5 1.880(10)
– O2 2.587(10)	– O2 1.897(9)
– O5 2.600(10)	– O7 2.656(11)
– O6 2.792(10)	– O3 3.000(12)
– O4 2.807(11)	– O6 3.065(12)
– O3 2.954(11)	– O4 3.237(12)
– S3 3.493(5)	– O8 3.299(15)
Pb2 – O1 2.557(9)	S1 – O4 1.463(17)
– O5 2.569(10)	– O7 1.479(12) × 2
– O5 2.601(10)	– O6 1.492(14)
– O2 2.730(10)	S2 – O3 1.459(10) × 2
– O3 2.862(12)	– O8 1.474(16)
– S3 3.029(4)	– S3 2.016(8)
– O8 3.045(9)	
– O7 3.079(14)	
- O7 3.168(13)	
- O1 3.310(9)	

https://doi.org/10.1180/mgm.2025.10143 Published online by Cambridge University Press

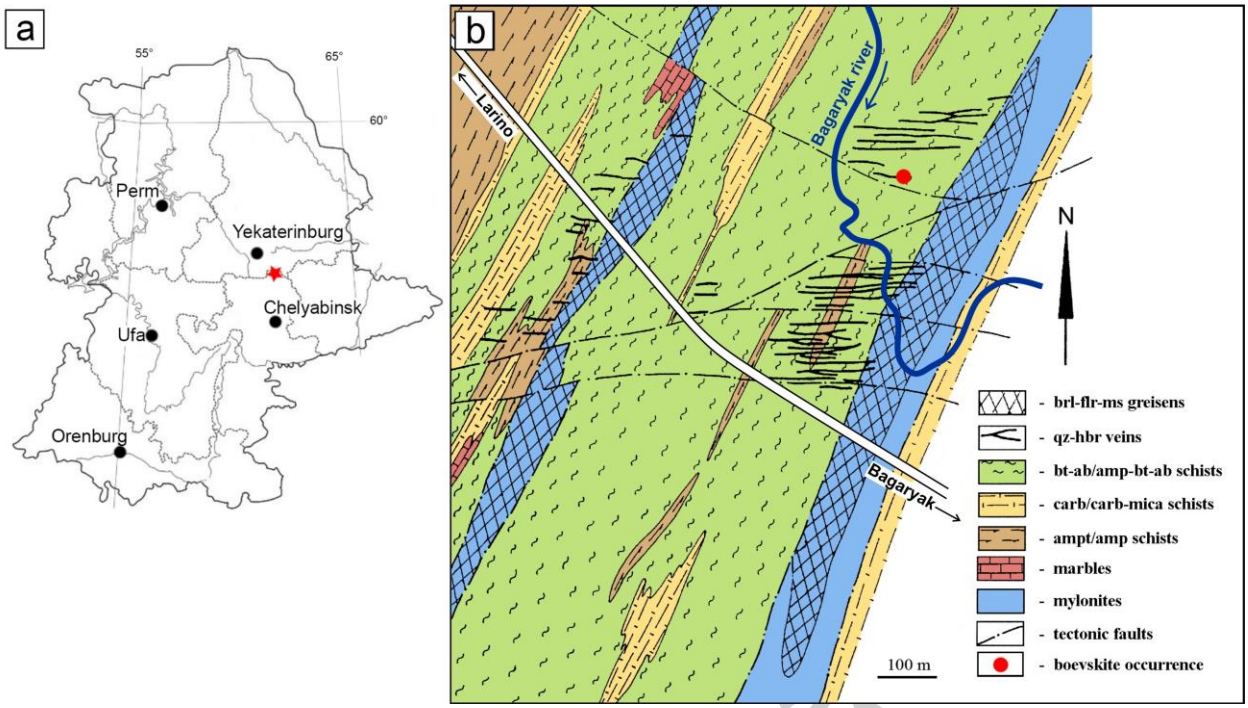

Figure 1: a) Geographical position and **b)** geological scheme of the Boevskoe deposit (drawn and modified after Zoloev *et al.*, 2004). Abbreviations: brl – beryl, flr – fluorite, ms – muscovite, qz – quartz, hbr – hübnerite, bt – biotite, ab – albite, amp – amphibole, carb – carbonaceous, mica – micaceous, ampt – amphibolite.

https://doi.org/10.1180/mgm.2025.10143 Published online by Cambridge University Press

Figure 2: a) The general view of the abandoned mine at the Boevskoe W-Be deposit. May 2023. Photo by Pavel Andrushchenko; **b)** collapsed adit on the border of which the specimens with boevskite were collected ("boevskite occurrence"); FOV 0.7 m. July 2023. Photo by Alexey Kuznetsov.

https://doi.org/10.1180/mgm.2025.10143 Published online by Cambridge University Press

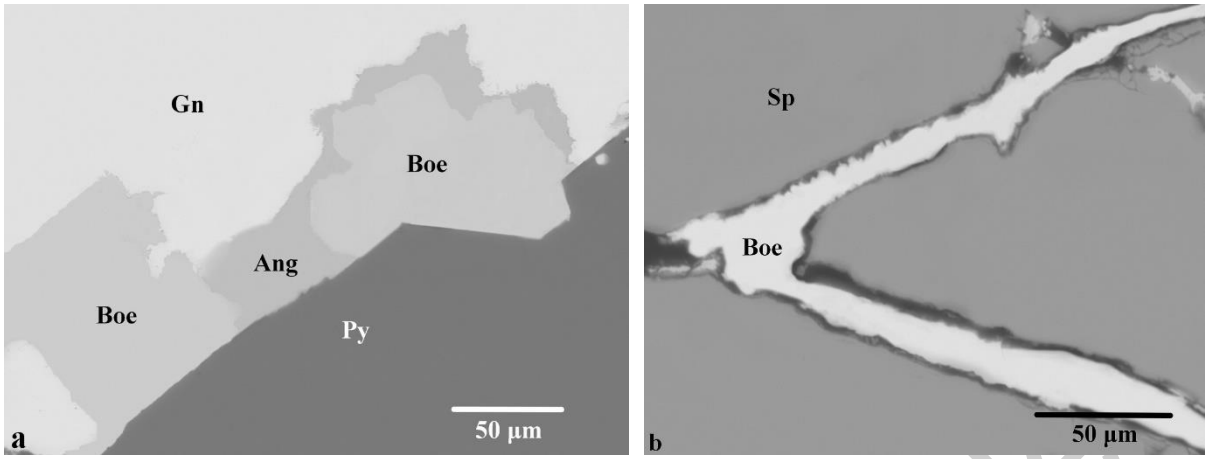

Figure 3: a – Boevskite (Boe) at the contact of galena (Gn) and pyrite (Py) with anglesite (Ang); **b** – boevskite veinlets in sphalerite (Sp). Polished section. SEM (BSE) images.

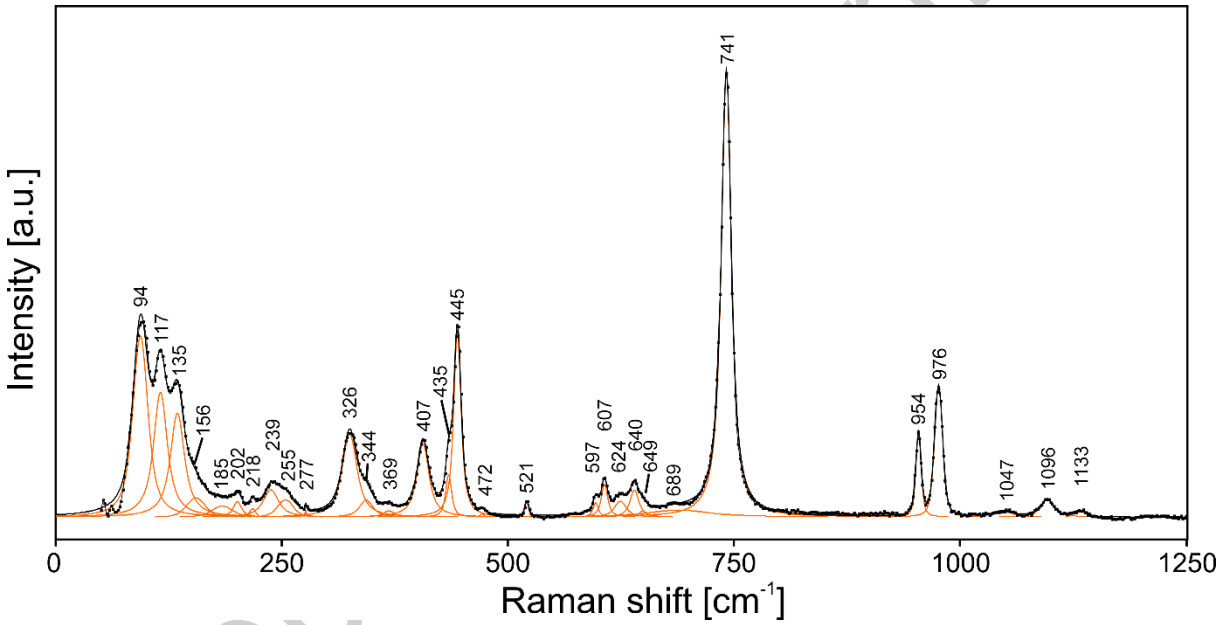

Figure 4. The Raman spectrum of boevskite excited by 532 nm laser in the 50–1250 cm^{-1} region. The measured spectrum is shown by dots. The curve matching to dots is a result of spectral fit as a sum of individual Voigt peaks shown below the curve.

https://doi.org/10.1180/mgm.2025.10143 Published online by Cambridge University Press

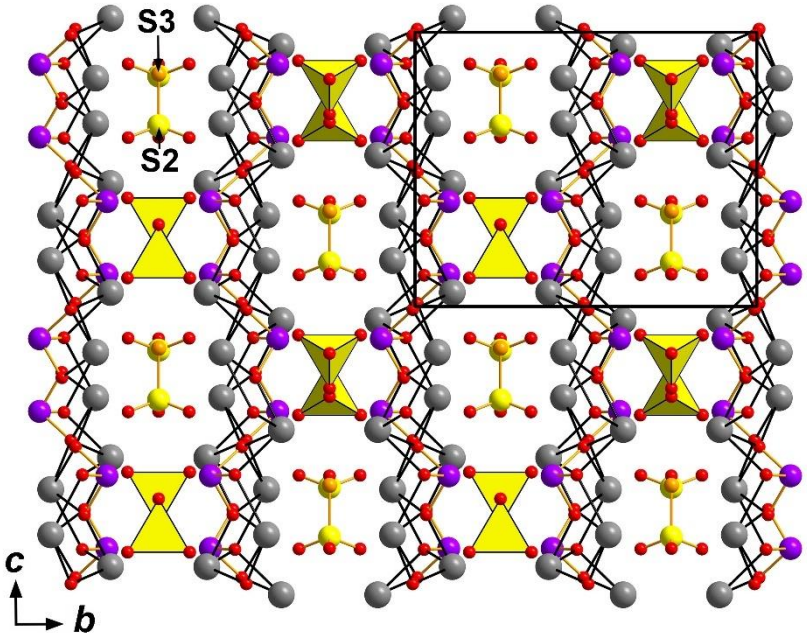

Figure 5. The crystal structure of boevskite projected along the *a* axis. Pb^{2+} cations are grey circles, Te^{4+} and O are lilac and red circles, respectively. SO_4 tetrahedra are yellow. S2 and S3 atoms of thiosulfate groups are large yellow and small orange circles, respectively. Only short (strong) Pb-O and Te-O bonds are shown. The unit cell is outlined.

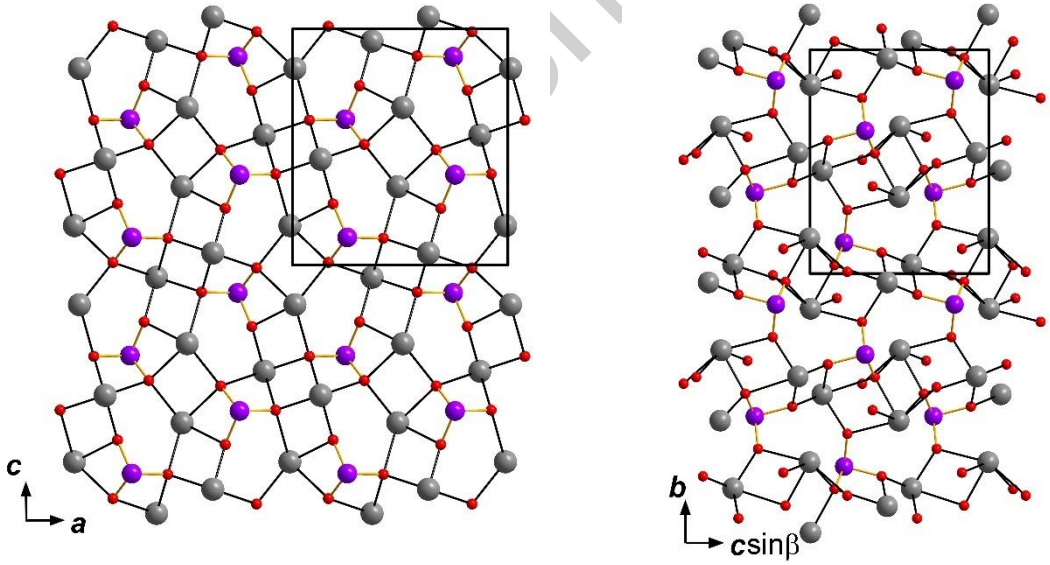

a

https://doi.org/10.1180/mgm.2025.10143 Published online by Cambridge University Press

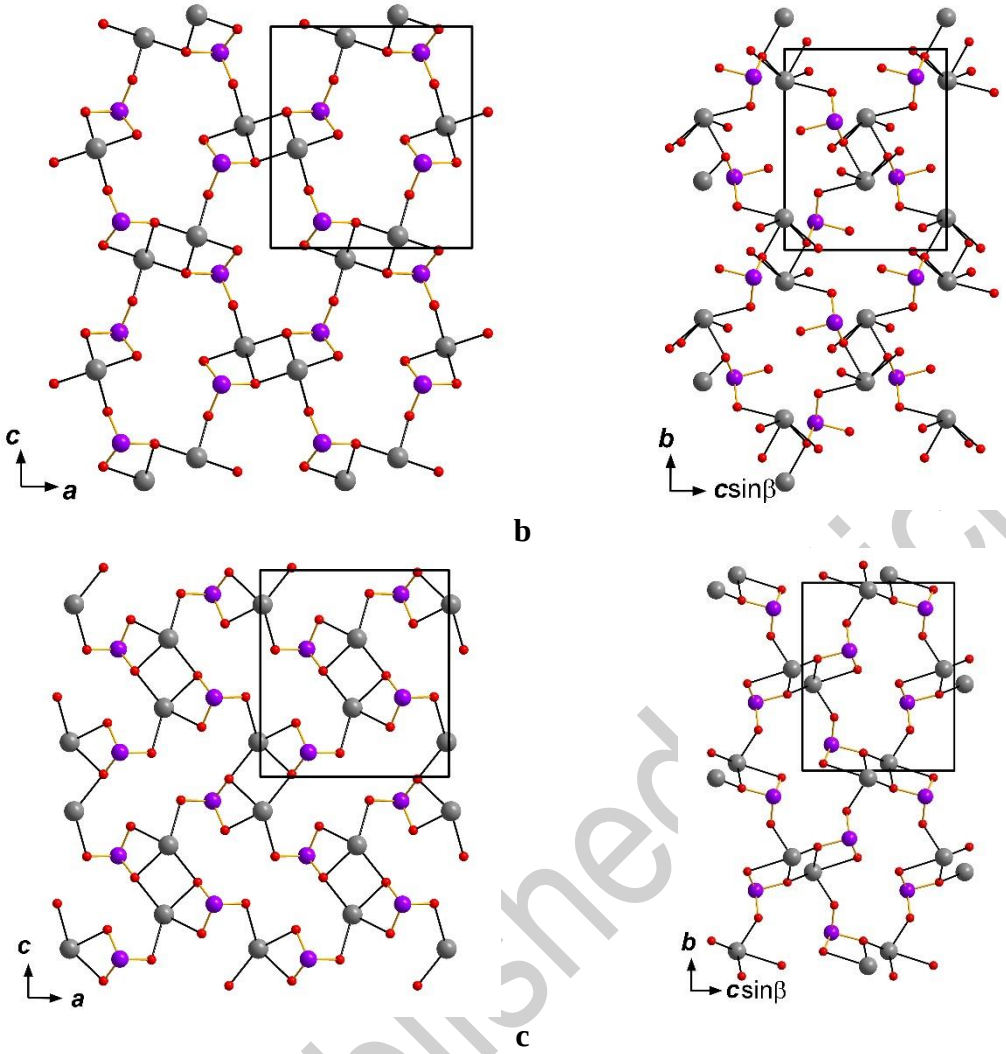

Figure 6. Te-Pb-O layers in boevskite (left column) and adanite (drawn after Kampf *et al*., 2020a; elongated Pb2–O bond 2.77 Å is included) (right column). Te-Pb(1,2)-O layer (**a**), Te-Pb(1)-O layer (**b**) and Te-Pb(2)-O layer (**c**). The unit cells are outlined.

https://doi.org/10.1180/mgm.2025.10143 Published online by Cambridge University Press